

Radiative Gaussian Splatting for Efficient X-ray Novel View Synthesis

Yuanhao Cai, Yixun Liang, Jiahao Wang, Angtian Wang,
Yulun Zhang, Xiaokang Yang, Zongwei Zhou, and Alan Yuille

Johns Hopkins University,
HKUST (GZ), Shanghai Jiao Tong University

- Introduction
- Method
- Experiment

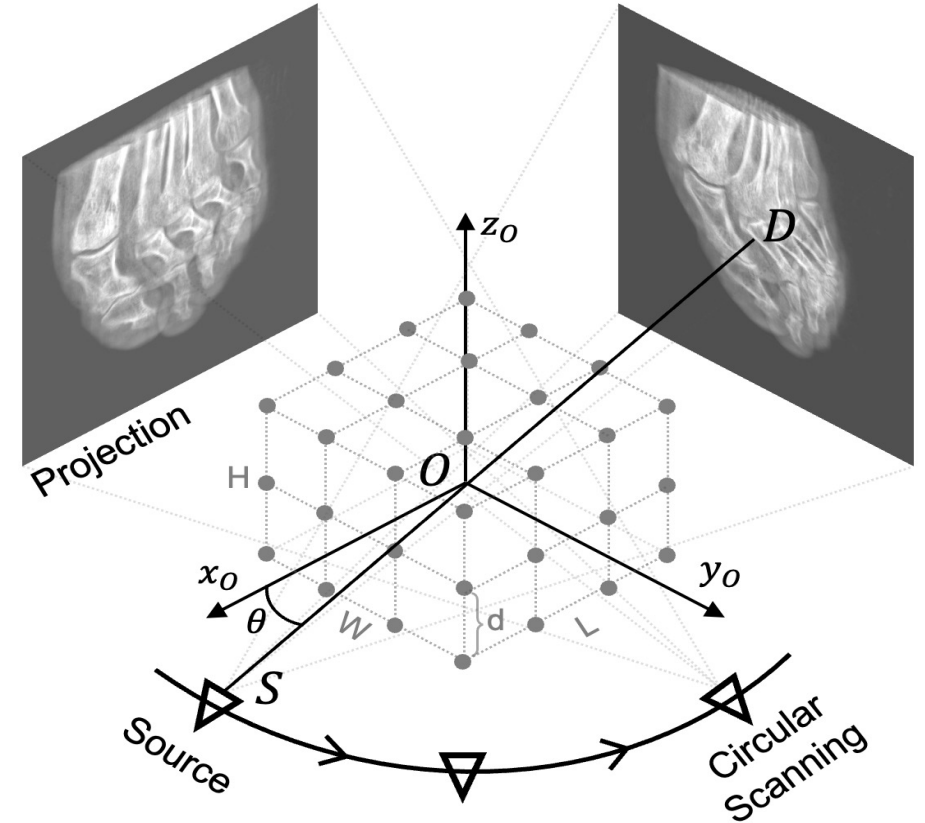
- Introduction
- Method
- Experiment

To reduce the harm of X-ray exposure, this work studies the low-dose X-ray reconstruction problem

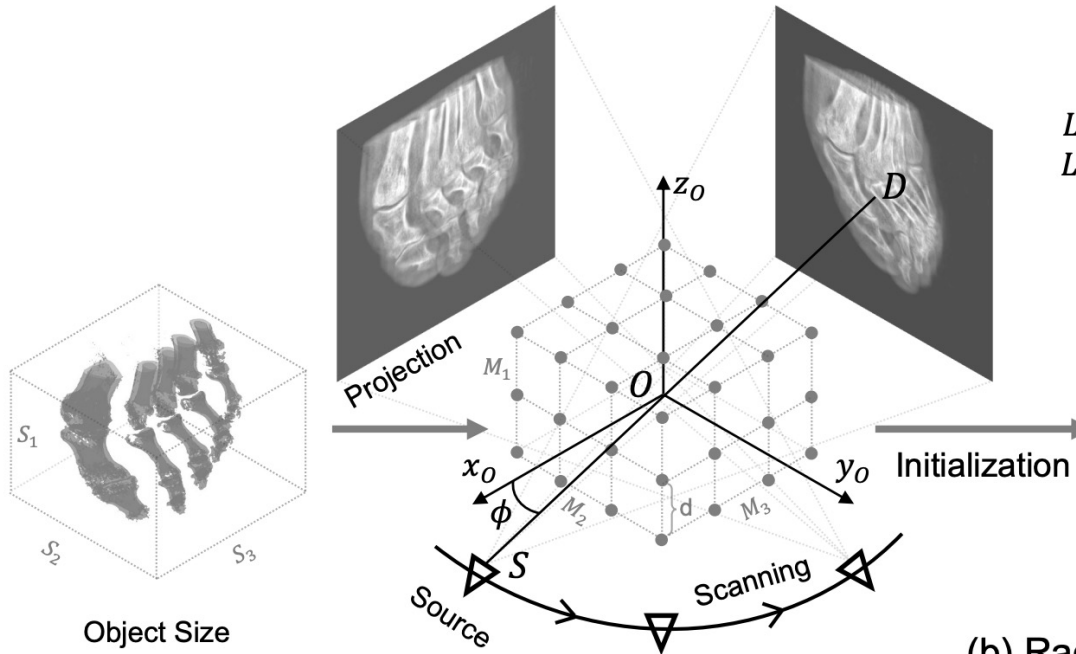
- X-ray Novel View Synthesis
- Computed Tomography Reconstruction

Natural light imaging is based on the reflection off the surface of the object → anisotropic, view dependent

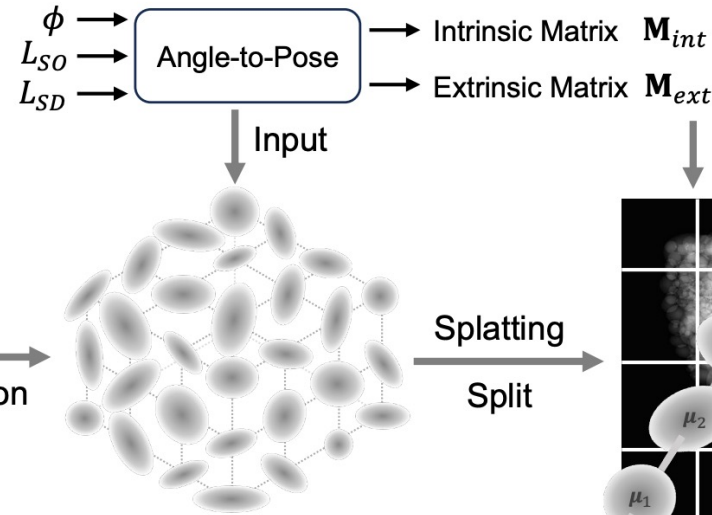
X-ray imaging is based on penetration and attenuation through the object → isotropic, view independent



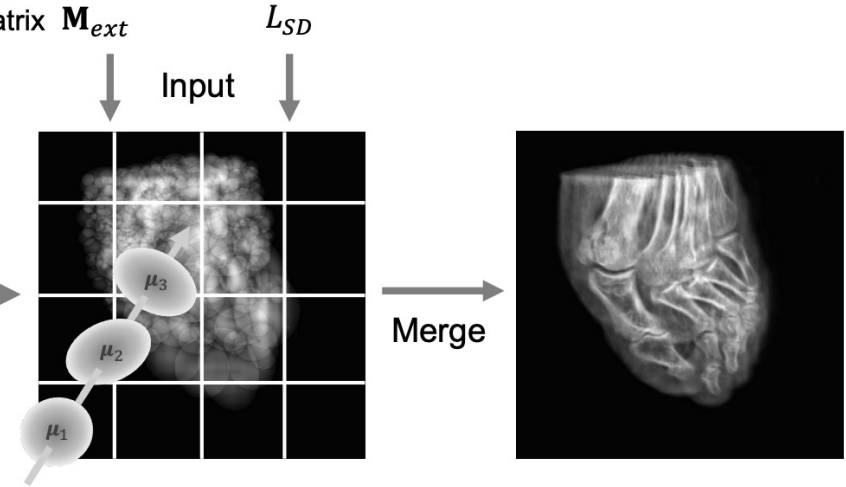
- Introduction
- Method
- Experiment



(a) Angle-pose Cuboid Uniform Initialization



(b) Radiative Gaussian Point Clouds



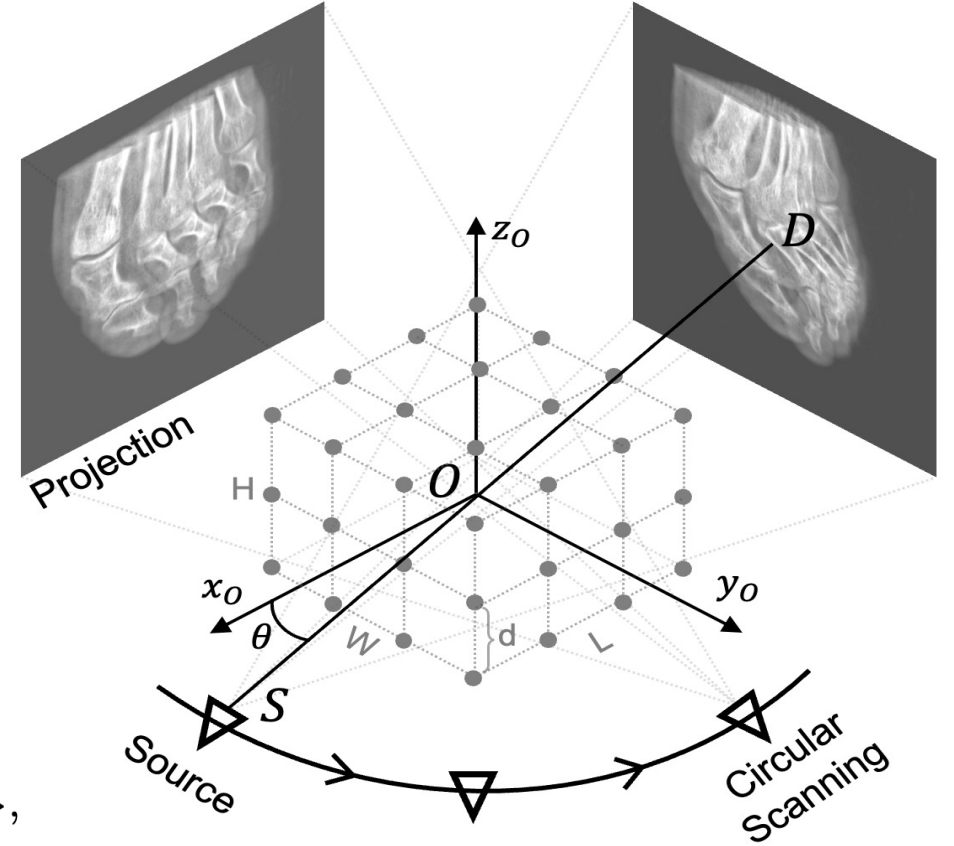
(c) Differentiable Radiative Rasterization

- Angle-pose Cuboid Uniform Initialization
- Radiative Gaussian Point Cloud Model
- Differentiable Radiative Rasterization

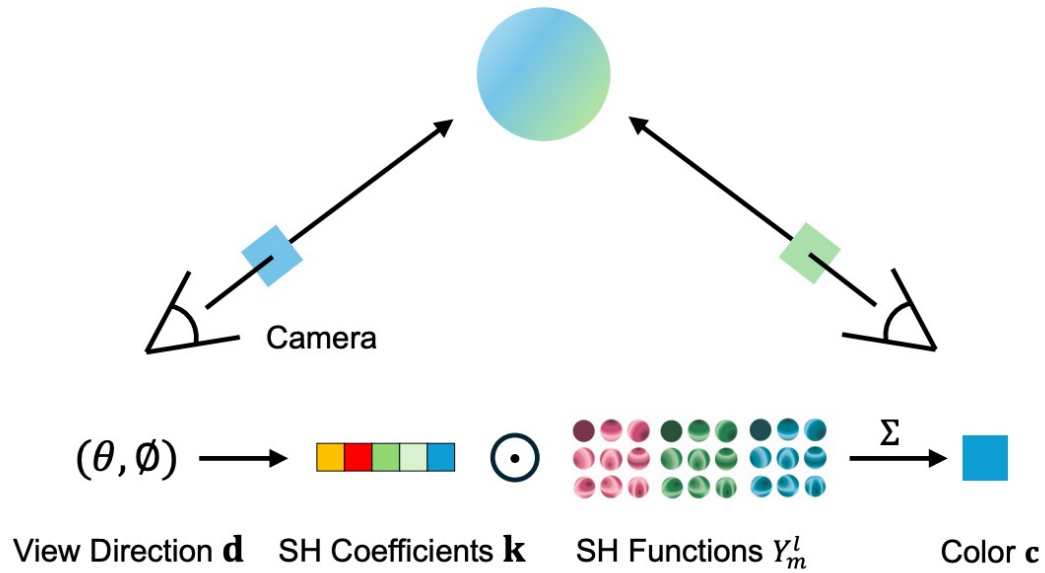
$$\mathbf{M}_{ext} = \begin{bmatrix} -\sin \phi & \cos \phi & 0 & 0 \\ 0 & 0 & -1 & 0 \\ -\cos \phi & -\sin \phi & 0 & L_{SO} \\ 0 & 0 & 0 & 1 \end{bmatrix},$$

$$\mathbf{M}_{int} = \begin{bmatrix} L_{SD} & 0 & W/2 & 0 \\ 0 & L_{SD} & H/2 & 0 \\ 0 & 0 & 1 & 0 \end{bmatrix},$$

$$\mathcal{P} = \left\{ \left(\frac{n_1 S_1 d}{M_1}, \frac{n_2 S_2 d}{M_2}, \frac{n_3 S_3 d}{M_3} \right) \mid -\left\lceil \frac{M_i}{2d} \right\rceil - 1 \leq n_i \leq \left\lceil \frac{M_i}{2d} \right\rceil + 1, i = 1, 2, 3 \right\},$$



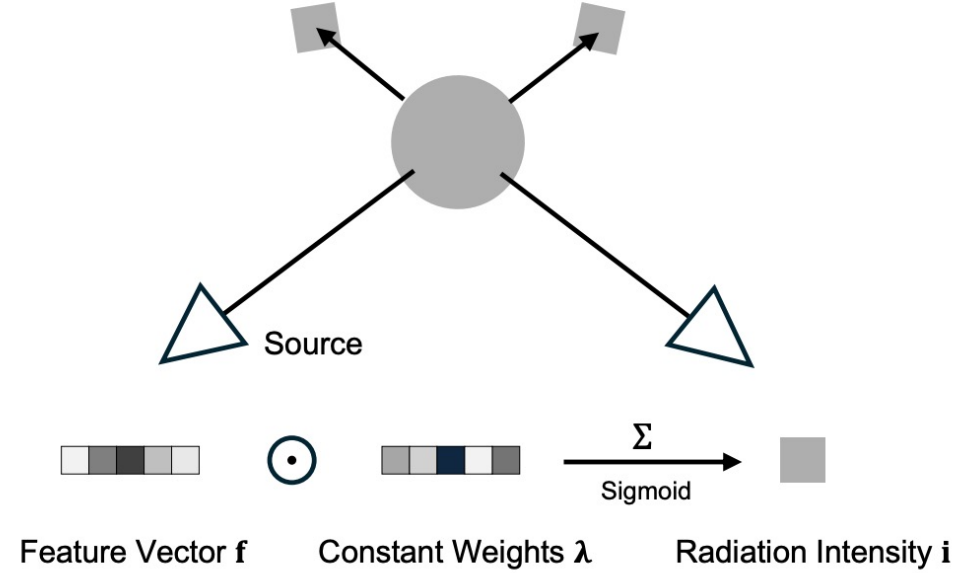
Our method is SFM-free !



(a) Original RGB Gaussian Point Cloud

$$\mathbf{c}(\mathbf{d}, \mathbf{k}) = \sum_{l=0}^L \sum_{m=-l}^l k_l^m Y_l^m(\theta, \phi),$$

Use Spherical Harmonics – view dependent



(b) Our Radiative Gaussian Point Cloud

$$\mathcal{G}_x = \{G_i(\boldsymbol{\mu}_i, \boldsymbol{\Sigma}_i, \alpha_i, \mathbf{f}_i) \mid i = 1, 2, \dots, N_p\},$$

$$\mathbf{i}(\mathbf{f}) = \text{RIRF}(\mathbf{f}) = \text{Sigmoid}(\boldsymbol{\lambda} \odot \mathbf{f}),$$

Radiation Intensity Response Function – view dependent

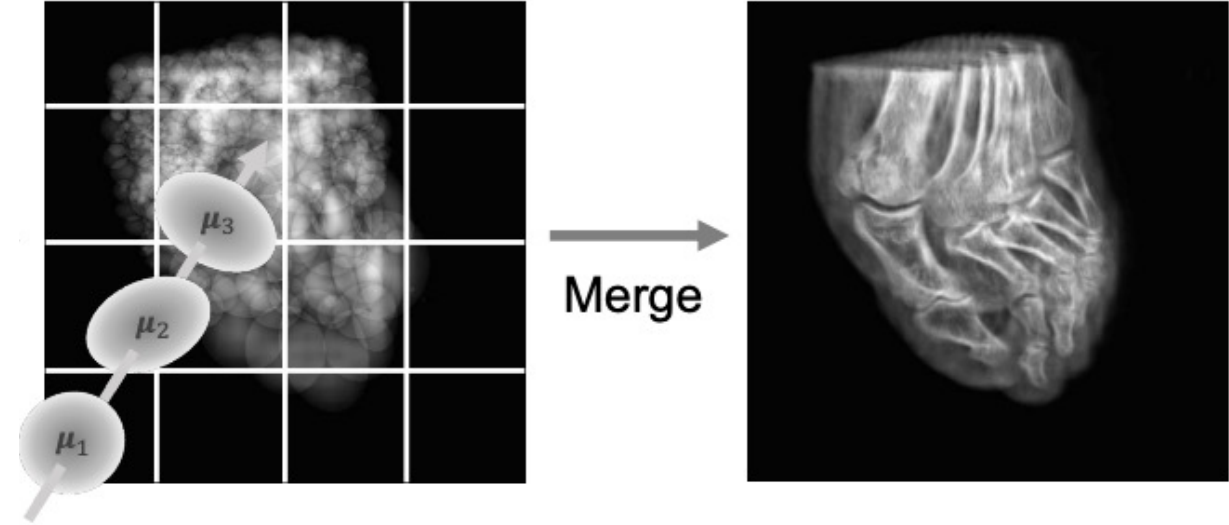
$$\mathbf{I} = F_{\text{DRR}}(\mathbf{M}_{\text{ext}}, \mathbf{M}_{\text{int}}, \{G_i(\boldsymbol{\mu}_i, \boldsymbol{\Sigma}_i, \alpha_i, \mathbf{f}_i) \mid i = 1, 2, \dots, N_p\}),$$

$$P(\mathbf{x}|\boldsymbol{\mu}_i, \boldsymbol{\Sigma}_i) = \exp\left(-\frac{1}{2}(\mathbf{x} - \boldsymbol{\mu}_i)^\top \boldsymbol{\Sigma}_i^{-1}(\mathbf{x} - \boldsymbol{\mu}_i)\right).$$

$$\tilde{\mathbf{t}}_i = \begin{bmatrix} \mathbf{t}_i \\ 1 \end{bmatrix} = \mathbf{M}_{\text{ext}} \tilde{\boldsymbol{\mu}}_i = \mathbf{M}_{\text{ext}} \begin{bmatrix} \boldsymbol{\mu}_i \\ 1 \end{bmatrix}, \quad \tilde{\mathbf{u}}_i = \begin{bmatrix} \mathbf{u}_i \\ 1 \end{bmatrix} = \mathbf{M}_{\text{int}} \tilde{\mathbf{t}}_i = \mathbf{M}_{\text{int}} \begin{bmatrix} \mathbf{t}_i \\ 1 \end{bmatrix},$$

$$\boldsymbol{\Sigma}'_i = \mathbf{J}_i \mathbf{W}_i \boldsymbol{\Sigma}_i \mathbf{W}_i^\top \mathbf{J}_i^\top,$$

$$\mathbf{J}_i = \begin{bmatrix} \frac{L_{SD}}{t_z} & 0 & -\frac{L_{SD}}{t_z^2} t_x \\ 0 & \frac{L_{SD}}{t_z} & -\frac{L_{SD}}{t_z^2} t_y \\ 0 & 0 & 0 \end{bmatrix}, \quad \mathbf{W}_i = \begin{bmatrix} -\sin \phi & \cos \phi & 0 \\ 0 & 0 & -1 \\ -\cos \phi & -\sin \phi & 0 \end{bmatrix},$$



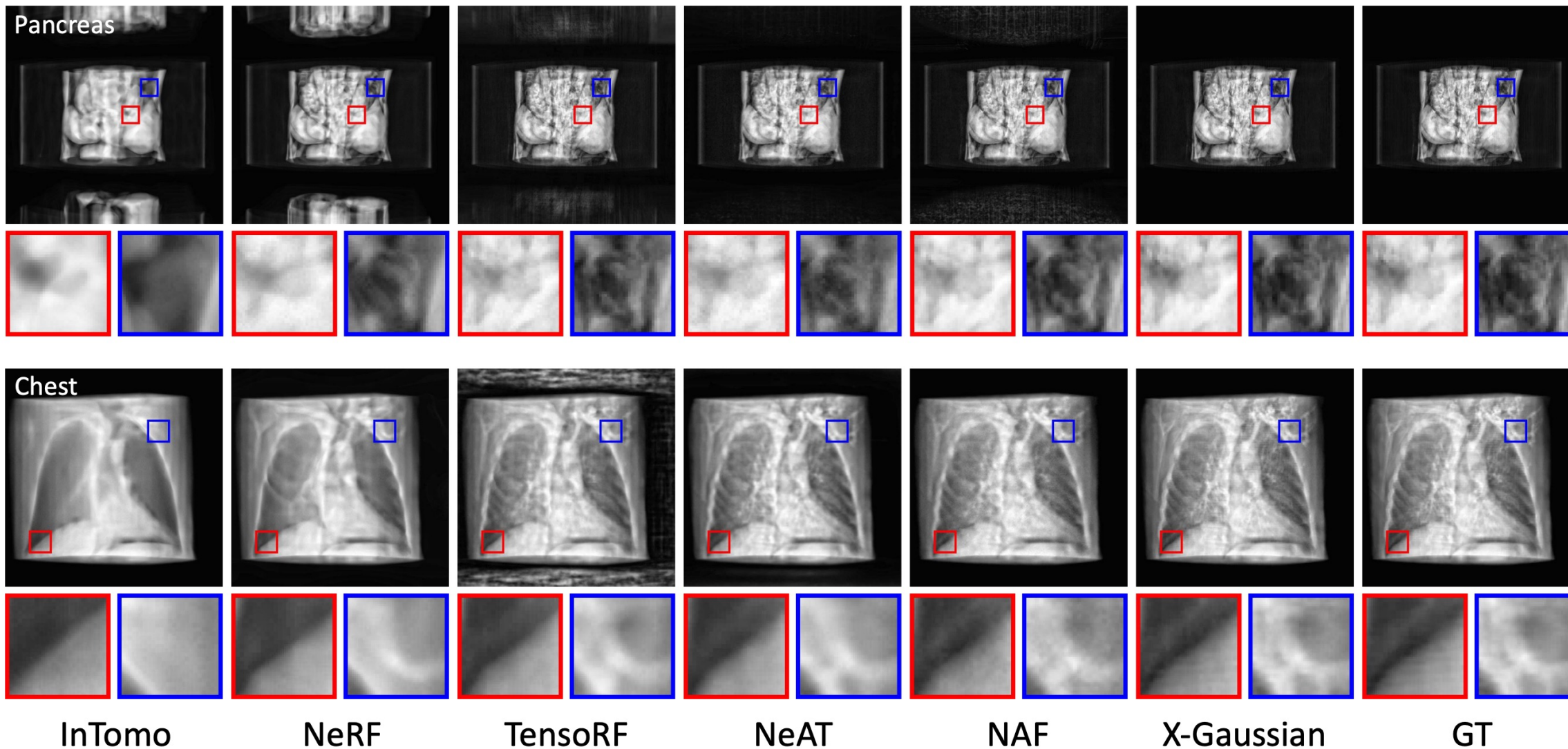
(c) Differentiable Radiative Rasterization

Image Coordinate System \rightarrow Camera Coordinate System \rightarrow World Coordinate System

- Introduction
- Method
- Experiment

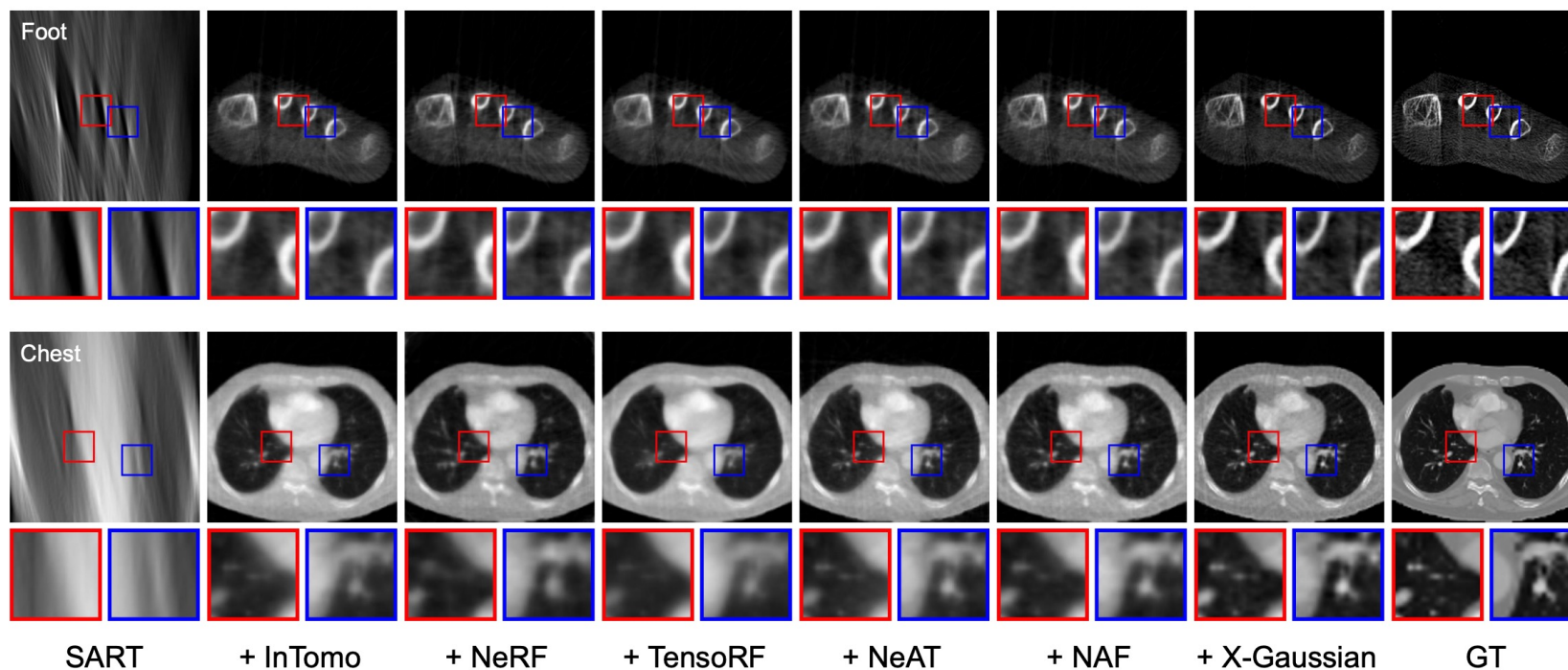
Method	Infer Speed	Train Time	Chest	Foot	Head	Abdomen	Pancreas	Average
InTomo [58]	0.62 fps	125 min	28.948 0.9915	39.482 0.9979	34.832 0.9977	27.641 0.9646	20.031 0.8537	30.187 0.9611
NeRF [37]	0.14 fps	313 min	36.157 0.9988	41.053 0.9989	29.760 0.9991	24.620 0.9559	19.853 0.8560	30.289 0.9617
TensoRF [10]	0.77 fps	178 min	23.609 0.9402	37.728 0.9929	34.429 0.9879	27.382 0.8730	29.235 0.8031	30.477 0.9194
NeAT [42]	1.78 fps	69 min	40.765 0.9990	38.236 0.9963	27.738 0.9295	26.741 0.8563	37.526 0.9017	34.201 0.9366
NAF [60]	2.01 fps	63 min	42.366 0.9993	38.353 0.9913	30.174 0.9531	37.590 0.9855	36.228 0.8844	36.942 0.9627
X-Gaussian	148 fps	9 min	43.887 0.9998	42.153 0.9997	41.579 0.9997	45.762 0.9999	43.640 0.9976	43.404 0.9993

On the novel view synthesis task, our X-Gaussian is 6.5 dB higher and 73 x faster in model inference speed.



Our X-Gaussian can reconstruct more structural details

Method	+ None		+ InTomo [58]		+ NeRF [37]		+ TensoRF [10]		+ NeAT [42]		+ NAF [60]		+ X-Gaussian	
	PSNR	SSIM	PSNR	SSIM	PSNR	SSIM	PSNR	SSIM	PSNR	SSIM	PSNR	SSIM	PSNR	SSIM
FDK	7.41	0.093	20.31	0.498	20.57	0.502	20.61	0.501	20.94	0.511	21.28	0.523	22.60	0.584
Δ FDK	0	0	12.90	0.405	13.16	0.409	13.20	0.408	13.52	0.418	13.87	0.430	15.19	0.491
SART	17.24	0.528	26.28	0.859	26.78	0.853	27.06	0.867	27.31	0.869	27.84	0.879	30.25	0.907
Δ SART	0	0	9.04	0.331	9.54	0.325	9.82	0.339	10.07	0.341	10.60	0.351	13.01	0.379
ASD-POCS	17.03	0.525	25.44	0.847	26.58	0.857	26.93	0.868	26.95	0.865	27.91	0.880	30.56	0.926
Δ ASD-POCS	0	0	8.41	0.322	9.55	0.332	9.90	0.343	9.92	0.340	10.88	0.355	13.53	0.401



On the sparse-view CT reconstruction task. Our method significantly boosts the performance of traditional methods By over 10 dB



Code, models, and data are publicly available at

<https://github.com/caiyuanhao1998/SAX-NeRF>